Santiago Escobar Nassar

DESIGN AND DEVELOPMENT OF AN ELECTRONIC INSTRUMENTATION DEVICE FOR HIGH-RESOLUTION MELTING CURVE ANALYSIS

MASTER´S DEGREE FINAL PROJECT

Supervised by: Ciara K. O´Sullivan and Mayreli Ortiz

MASTER´S DEGREE IN NANOSCIENCE, MATERIALS AND PROCESSES: CHEMICAL TECHNOLOGY AT THE FRONTIER

UNIVERSITAT ROVIRA I VIRGILI

Tarragona
2016

Design and development of an electronic instrumentation device for high-resolution melting curve analysis

Santiago Escobar Nassar

Master program in nanoscience, materials and processes 2015 – 2016

E-mail: santiago.escobar@estudiants.urv.cat

Supervisors: Ciara K. O´Sullivan and Mayreli Ortiz

Department or Chemical Engineering, Universitat Rovira I Virgili

Campus Sescelades, Av Països Catalans, 26 Tarragona, 43007, Spain.

Abstract. The design and development of a computer-controlled heating block is reported. This unit is part of a novel electronic instrumentation system, specially designed for electrochemically marked high resolution melting curve analysis and intended to be used for the multiplexed detection of SNPs and mutations. The system herein explained, consists of a pair of aluminum blocks that are heated in a controlled way using a pulse width modulation protocol implemented on an Arduino UNO. Data processing and temperature control at different heating resolutions was performed via a proportional integral controller, also implemented on the Arduino. Heating tests using as template a glass slide with PMMA (setup that simulates the behavior of real electrodes) were performed to validate the system functionality and performance. Furthermore, a 1 and 13 gold electrode arrays were modified with a double thiolated covalently linked polyT single stranded DNA. Afterwards, the system was incubated with a polyA chain labelled with horseradish peroxidase (HRP). This system was exposed to a tetramethylbenzidine dihydrochloride (TMB) and hydrogen peroxide (H_2O_2) solution to determine the best electrode coverage ratio. A fast chonoamperometric test was carried out to determine the best probe/backfiller ratio for forthcoming experimentations on a model DNA sample.

I. INTRODUCTION

The completion of the human genome project has led to an important breakthrough in science due to the fact that its findings had contributed to expand and elucidate our understanding of the genome. One of the most important contributions was the complete sequencing and mapping of all the human DNA coding and non-coding regions [1]. Within all this regions, different mutations and single nucleotide polymorphisms (SNPs) have been detected and studied. Mutations, on one hand, are defined as changes in the gene or chromosome structure caused by any base deletion, insertion or exchange between parent DNA strands. These mutations can be categorized in homozygotes (change of a base pair between strands keeping complementarity) or heterozygotes (change in a base pair that produces non-complementarity) [2]. Regarding SNPs, these are single nucleotide variations that are present in specific sections of the introns. 99.9% of the human genome contains the same SNPs. However, with the development and enhancement of different techniques for genotyping and sequencing, scientists have discovered that 0.1% of our genome contains SNPs that vary from each individual. Furthermore, this SNPs contain information that not only defines some phenotypical attributes, but their study plays an important role for the progress of personalized medicine, patient stratification and base line disease detection [3].

SNPs and mutation detection can be carried out by different methods and techniques. Some examples of conventional techniques used for mutation scanning are: denaturing gradient gel electrophoresis [4], temperature gradient capillary electrophoresis [5], and denaturing high performance liquid chromatography [6]. However, all this methods depend on expensive equipment [6, 7], and undergo a time consuming separation step of the PCR product into gels or other matrixes. This step represents a necessary but counterproductive task that might compromise the complete experiment due to sample contamination as a consequence of the environment exposure [8]. Alternatively to this techniques, current methods for mutation and SNPs detection are performed by melting curve analysis. All the methods mentioned above rely on determining the melting temperature of double stranded DNA (dsDNA) [2, 6-22]. The melting temperature (Tm) is an intrinsic characteristic of dsDNA and defines the temperature where 50% of the DNA has denatured or melted into single stranded DNA (ssDNA).

Melting curve analysis is mainly performed by two methods: fluorescence and electrochemical detection. The former uses probe DNA that can be either in solution or immobilized onto a surface. Along with this, either radioactive, enzyme-based, fluorescent or luminescent dyes or luminescent intercalators that binds to the dsDNA are used. By heating the solution or the electrode, the dsDNA will start to denature, releasing the marker and changing its fluorescence intensity. This change is recorded in real-time by a CCD camera [15] or by specialized instruments like the LightCycler [7, 8, 16, 22-24] LightScanner [14, 23, 24] or the HR-1 from Idaho technology [6, 7, 16, 22-24]. Although, fluorescence detection has a significant limitation: the background effect of the fluorescent dye, that even though it can be eliminated with exponential background subtraction [24], it will hinder homozygote detection [2].

In the case of electrochemical detection, it implements electroactive moieties and/or electroactive intercalators that binds to the target ssDNA or to the dsDNA that forms between the target and the complementary probe immobilized on the surface. Once they bind, the close proximity of the moieties to the conductive electrode promotes the electron transfer onto the surface. Temperature ramping is used to induce DNA dissociation, which increases the distance between the marked dissociating

strand and the electrode (or liberates part of the intercalators), along with the concomitant intensity reduction that can be read from the electroactive moieties signal. This electrochemical variation can be recorded using differential pulse voltammetry (DPV) and a specialized software like LabView, GPES, or NOVA for data recollection [9, 11, 13, 18-20]. Electrochemical detection is considered as one of the most attractive alternative for homozygote, heterozygote and SNPs detection. This is because it allows to directly obtain the melting curves and Tm with cost-effective instrumentation and without the need for image processing [19]. Furthermore, it shows high compatibility and flexibility with current miniaturization techniques for electrode and equipment development without this compromising on the overall sensitivity or specificity [19]. However, one important limitation regarding the use of electroactive intercalators is that some of them present a non-specific and weak interaction that makes it prone to be easily washed during the melting curve analysis. The methylene blue (one of the mostly used electrochemical intercalators) for example, presents different interactions with the dsDNA like: intercalation within the strands, electrostatic attraction with the DNA backbone and a high affinity to free guanines present in ssDNA [19]. This results in a weak and non-specific interaction of the methylene blue with the DNA or with an electrostatic interaction with any other charged particles. To overcome the problems of lack of specificity and intercalator leakage, some reports have studied the incorporation of modified nucleotides with functionalized electroactive markers into the target DNA during PCR. Some examples of this are with the use of nitrophenil, aminophenil, [25] benzofurazane [26], or phenothiazine (PTZ) [27].

Regardless of the detection method (fluorescence or electrochemical), heterozygotes can be detected by comparing the melting curve shape. On the other hand, homozygotes tend to change the melting curve Tm. Different reports have determined that 84 % of homozygote mutations and SNPs will shift the Tm around 0.5 °C[6] and by 1 °C for small amplicons [7]. However, if base exchange between the strands and base pair is preserved along with the neighbor complementarity, the change in the Tm becomes smaller (<0.4 °C) or even undetectable [6, 7, 22]. In order to correctly detect this mutations, the resolution of the melting curve instruments needs to be enhanced. High-resolution melting curve analysis (HRMCA) comes as the best suited solution for this problem. Its resolution depends on the heating rate of the heating system and on the detection rate of the data acquisition system. Commercial instruments like the HR-1 or the LightCycler allows to have controlled heating ramps of 0.3 °C/s and 0.05 °C/s, respectively [23, 24]. Nevertheless, they are expensive equipment, with prices ranging from $ 50000 down to $ 15000 [7]. Another major problem is that there are not HRMCA systems available in the market that are especially suited for electrochemical assessment.

Taking into account all the aforementioned, the design and development of a computer-controlled heating block is

herein reported. This unit is part of a novel electronic instrumentation system, specially designed for electrochemically HRMCA and intended to be used for the multiplexed detection of SNPs and mutations, see Figure 1. The main outcome herein explained, is a system that allows the user to select from different resolutions: 0.2 °C/step, 0.5 °C/step and a maximum of 1 °C/step even whilst the melting curve is in process. A couple of power BI BPC10 680 J resistors will heat a pair of aluminum metal plates where the sample electrodes should be placed in between (ensuring temperature homogeneity on all samples). A Proportional Integrative (PI) control algorithm was implemented to ensure a fine and robust control of each of the heating resolutions. For the temperature readout from each of the metal plates, commercial K type thermocouples were used. All the information was delivered and processed by an Arduino UNO board using the free Arduino software for data visualization and interaction with the user. Some heating tests, starting from 25°C to 90°C with all three resolution options, were performed on a glass slide with PMMA in order to validate the system´s functionality and performance. Additionally, an initial work with the electrodes that will be used for a HRMCA with a model sample was performed. A 1 and 13 gold electrode arrays were used to determine the best capture probe/backfiller ratio using different proportions of thiolated covalently linked polyT ssDNA and an alkyl thiol as the backfiller. Then, a polyA-HRP ssDNA and a TMB solution was used as a reported system. The work should continue with the electrode modification with ssDNA capture probes using the optimized probe/backfiller ratio. Afterwards, the electrodes need to be incubated with the modified target ssDNA sequence.
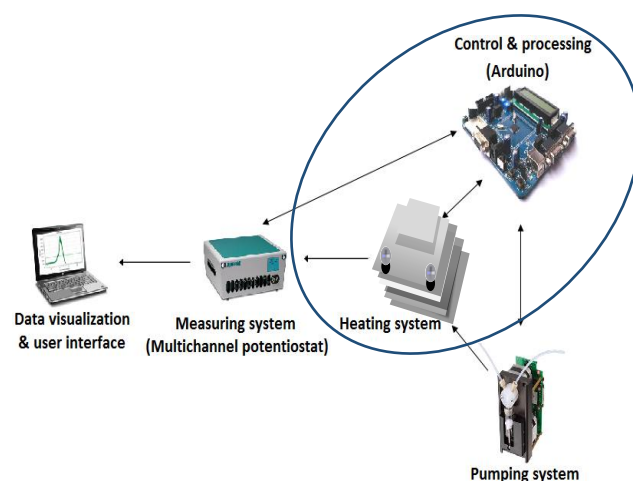
Figure 1. Scheme of the complete electronic instrumentation system highlighting the developed subsystem.

II. EXPERIMENTAL SECTION

A. Electronic components

The Arduino UNO, IRF520, the 16x2 LCD screen, the resistances, condensers, type K thermocouples, connectors, the BI BPC10 resistors, AD595, breadboard, and the 2.5W/mK thermally conductive tape were all purchased from Farnell (Madrid, Spain).

For the temperature reference system, a type K thermocouple connected to the precision thermometer Hi 93531 (Hanna instruments, Bilbao, Spain) was used. The variable DC power supply PeakTech 6006D (Telonic instruments LTD, Berkshire, UK) was used to supply the temperature reading system at 5.1 V.

B. Heating system characterization

1) Transfer function

For the system characterization a type-k thermocouple and a BI BPC10 680 J resistor were attached using the conductive tape to each of the heating blocks. To determine the step response of each system, a 0.48 mV step was applied to each resistor. All the temperature readings were recorded with the Arduino and with the Matlab 2013a software, the system behavior was modelled. An inspection to each response, revealed that both corresponded to a type I system. Using Matlab, the process gain Kp, the t1 and t2, which correspond to the time when the output attains the 63.2 and 28.3 percent of its final value, respectively, were defined. With this parameters obtained, it was possible to calculate for each system the theta (θ) and tau (τ) variables, along with the continuous time transfer function in the Laplace domain. The theta, tau and type I plus dead time continuous transfer function can be calculated as follows.

$$\tau = \frac{3}{2} * (t_2 - t_1)$$

$$\theta = t_2 - \tau$$

$$G_p = \exp(-\theta * s) * \frac{K_p}{(1 + \tau * s)}$$

2) PI tuning

For the PI tuning, the Matlab tool Simulink was used to model the closed loop response of each PI controller in series with a heating plate. The transfer function of each plate was needed in order to have the correct model of the system behavior. With the Simulink tool PID tuner, it was possible to tune and observe the closed loop response and reference tracking of each system as well as the error, the controller effort, the open loop response, plus many other options. For the PI control system the following equation was used:

$$C_{out} = K_c * e(t) + K_i * \int e(t)dt$$

Were e (t) represents the error or what is the same, the setpoint – input, Cout is the controller output, Kc is the proportional gain and Ki represents the integral gain.

3) Heating tests

To validate the systems functionality the following heating test was performed: as a template to simulate the behavior of the real gold electrodes, a glass slide with a microfluidic section made out of PMMA placed on top was used. To monitor the temperature stability and evolution though time, a thermocouple was glued on top of the glass slide using the

thermoconductive tape. This setup was placed in the middle of the heating blocks and sealed in a plastic casing for room temperature isolation. The temperature readings where registered with the Arduino and compared with another thermocouple placed as reference on each plate. This was also to contrast the system behavior with the reference and to apply, if needed, the correspondent temperature corrections. One end of the BI BPC power resistors is connected to a 24 V DC adapter and the other end to the drain of an IRF520 power transistor. These transistors are responsible to deliver a controlled current to each of the resistors. The power delivered by each IRF was modulated through the duty cycle variation of a 10 bit pulse width modulation (PWM) system implemented on an Arduino UNO. The PWM worked at a frequency of ~4 KHz at 5 V. Finally, the glass slide and reference readings were recorded using the Hi 93531.

C. Chemicals and materials

Solutions were prepared using a Milli-Q water purifier system (Milipore, Madrid, Spain) with a resistance level of 18.2 MΩ*cm^{-1}.

The chemicals and reagents were of analytical grade and used without further purification: potassium dihydrogen phosphate KH_2PO_4, acetone, isopropanol (Scharlau), potassium hydroxide KOH, hydrogen peroxide H_2O_2 30% (v/v), potassium ferricyanide $K_3[Fe(CN)_6]$, dithiol-(16-3,5-bis ((6mercaptohexyl)oxylphenyl)-3,6,9,12,15-pentaoxahexa-decane (DT1) and tris buffer at 7 pH (Sigma Aldrich, Tres Cantos, Spain). For the Tris buffer the pH was adjusted to 7 using HCl 1 M and NaOH 1 M (Sigma Aldrich)

The HRP substrate formulation 3,3′,5,5′-tetramethylbenzidine (TMB) enhanced one component HRP membrane (TMBr 0.05 %, w/v) was purchased from Diarect AG (Germany).

Three millimeter thick polymethylmethacrylate (PMMA) was purchased from *La Industria de la Goma* (Tarragona, Spain) and the double-sided adhesive foil ARseal^{TM} 90880 was purchased from Adhesive Research (Ireland).

Thiolated polyT and polyA-HRP oligonucleotides were purchased as lyophilized powder from Biomers.net (Ulm, Germany), reconstituted in milli-Q water (18MΩ) and used without further purification. Table 1 shows a detailed description of the DNA samples used in this study,

Table 1. Details of the oligonucleotides used in this study. The capture probe is 32 mer to increase the immobilizing stability.

Thiolated polyT capture probe (32 mer)	5'-GTCGTGACTGGGAAAACTTTTTT TTTTTTTTT-3'
PolyA-HRP (15 mer)	HRP-5'-AAAAAAAAAAAAAAA-3'

D. Gold electrodes

Two different gold electrodes fabricated on glass substrate were used (Figure 2).

a) **1 gold electrode array**: 2.9 x 2.5 x 0.1 cm Au electrode with a working electrode surface of 12.56 mm^2. Produced by IMM

b) **13 gold electrode array**: 4.3 x 2.5 x 0.1 cm 13 electrode array with a working electrode surface of 0.95 mm^2. Produced in the clean room facilities of Rovira i Virgili according to protocol described by Sabate del Rio et al [29].
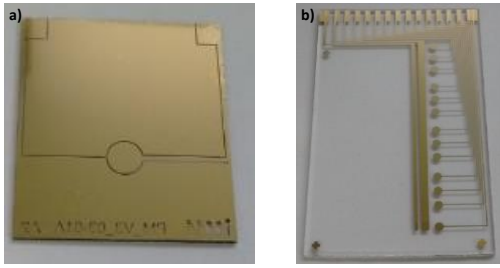
Figure 2. (a) 1 gold electrode array (b) 13 gold electrode array composed of 13 working electrodes, a block counter and a block reference.

2) Gold electrodes cleaning

All arrays were first sonicated in acetone for 5 minutes. Next step was to sonicate in isopropanol for 5 minutes. Following this, all electrodes were rinsed with Milli-Q water and then sonicated for 10 minutes in a solution 50mM of KOH and H_2O_2 30% in a ratio of 3:1. Finally the electrodes were dried with an N_2 spray gun.

3) Electrode modification

For the electrode modification the following protocol was followed.

Table 2. Ratios and concentrations of immobilization cocktails tested for probe immobilization.

	Ratio 1:1	Ratio 1:10	Ratio 1:20	Blank
	c(µM)	c(µM)	c(µM)	c(µM)
polyA-HRP	50	5	5	0
DT1	50	50	100	100
KH_2PO_4	10^6	10^6	10^6	10^6

The working electrodes in the 1 and 13 electrode arrays were dropcasted with 4 µl and 1 µl of immobilization cocktail respectively. Then, all electrodes were placed on a humid chamber inside an incubator and left for three hours at 37 °C.

After incubation all the arrays were washed in tris buffer for 1 minute under agitation, twice. Finally all electrodes were dried with the N_2 spray gun.

4) Incubation with poly T - HRP.

A solution of fresh poly T – HRP was prepared by mixing 99 µl of tris buffer with 1 µl of poly T – HRP at 1 µM. 40 µl were used to immobilize on the 13 electrode array and 4 µl on the 1 array to cover the entire area of the working

electrode. All electrodes where placed on a humid chamber and inside an incubator (New Brunswick scientific, USA) at 37 °C for 30 minutes.

To remove the excess solution from the 13 electrode array, it was washed with 600 µl of Tris buffer and spayed with the N_2 spray gun. For the 1 electrode array it was immersed in tris buffer at room temperature, then washed under agitation in fresh Tris for 1 minute. Finally it was dried with the N_2 spray gun.

5) Incubation with TMB

For the TMB incubation, 50 µl of TMB was placed on the 13 electrode array and 20 µl on the 1 array. They were both left for incubation for 10 minutes at room temperature.

E. Electrochemical measurements

All electrochemical measurements where performed using an Autolab model PGSTAT 12 potentiostat/galvanostat controlled with the software NOVA 2.0 (Eco Chemie B.V, Netherlands). For both arrays a three electrode configuration was used with the reference, working and counter electrode made out to gold.

1) Fast chronoamperometric measurements

All fast chonoamperometric measurements consisted of a 2 step process. In the first step, no voltage is applied within 0.01 seconds and with an interval time of 0.1 ms. In the second step a potential of -0.2 Vref is applied with a 0.5 seconds of duration and with an interval time of 0.1 ms.

2) Cyclic voltammetry measurements

The cyclic voltammetry measurements were conducted with an unstirred solution of 2 mM of $K_3[Fe(CN)_6]$ with a start potential of 0 V, an upper vertex potential of 0.6 V, a lower vertex potential of -0.6 V and a stop potential of 0 V. Finally a 0.1 V/s scan rate was used with steps of 2.44 mV.

III. RESULTS AND DISCUSSION

A. Transfer function

In the complementary information are shown the results obtained from the transfer function experiments carried on the heating block 2. The resulting transfer functions are:

Heating plate 1:

$$G_{p1} = e^{(-6.08*s)} \frac{0.449}{252.3 * s + 1}$$

Heating plate 2:

$$G_{p1} = e^{(-7.18*s)} \frac{0.553}{272.3 * s + 1}$$

Figure 3 shows the step response of the modelled transfer function of the heating block 1. In this figure is clear that the model is in concordance with the system behavior, what allows to use this transfer function to model and study the closed loop response of the PI controller in series with the system.
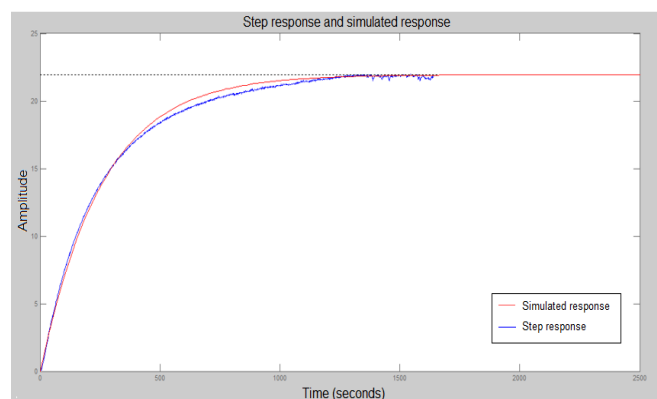
Figure 3. Step response and simulated transfer function of the heating block 1 obtained with Matlab.

B. PI tuning

To control the resolution of each of the heating blocks, a control algorithm is necessary. There are different kinds of controllers in the market, being the PID the most common and the first and most recommended of all. This is because the proportional part improves the rising and settling time of the response. The integrative part reduces the steady-state error and the derivative part is used to reduce both the overshoot and the change rate of the error. For all these reasons, the PID is the most recommended option for system control. Nonetheless, the PID might not be the most suitable solution for every system. This will depend on many factors like the control variable, the type of system, the type of response needed (to be underdamped, overdamped, or critically damped in type II systems for example), the overshoot acceptance level, the settling time and the controller effort.

In the particular case of a heating system that wants to control a resolution of 0.2 °C/step and were the slightest variation of the temperature might produce the DNA dissociation and a Tm change, it is important to minimize to the maximum the steady-state variation of the system. The problem with using a PID in this case is because the differential part tends to inhibit rapid movements of the output. This implies that if the derivative parameter has a high value it might amplify the noise, reflecting this in the controller output to keep on the set point. Taking into account all the aforementioned, the proportional integrative control shows to be more suitable for this case.

By using Simulink, both control-heating blocks were modelled and with the PID tuner, the correspondent Kp and Ki values were tuned to produce a system response with a fast rising and settling time, and with the minimum or no overshoot. Figure 4 shows the modelled PI system in series with the heating block 1 in Simulink. Figure 5 shows the simulated closed loop response.
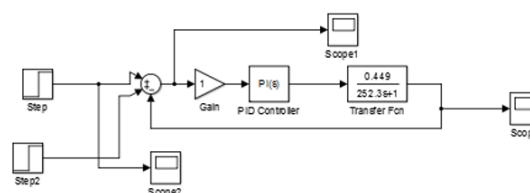
Figure 4. Modelled system of the PI controller in series with the transfer function block that simulates the behavior of the heating plate 1. Two steps where implemented as input to simulate and observe the system response to a change in the set point.

The best Kp and Ki parameters that produced the best response on both heating blocks were 55.85 and 1.33, respectively. This variables allowed to have a rise time of 15.6 seconds, a settling time of 1 minute and 50 seconds, and a 10.4% overshoot. The latter parameter in principle is unacceptable because with each change on the set point, the temperature would overpass this set point and produce an unwanted change on the DNA. However, when the heating experiments were carried out on the real system, the output never exceeded the set point. One possible explanation for this is that the simulation was made with a step response of 1 V, although, the highest voltage change made by the PWM in order to increase the block temperature by 1 °C is 24.41 mV. This means that the input shift might not be that drastic to produce such a response on the controller.
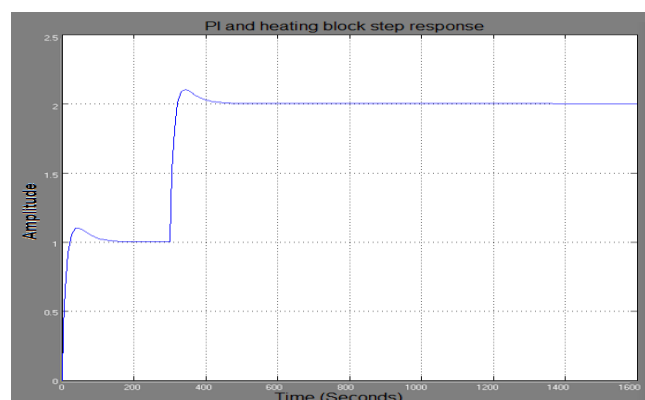
Figure 5. Modelled closed loop response of the PI controller in series with the heating block 1.
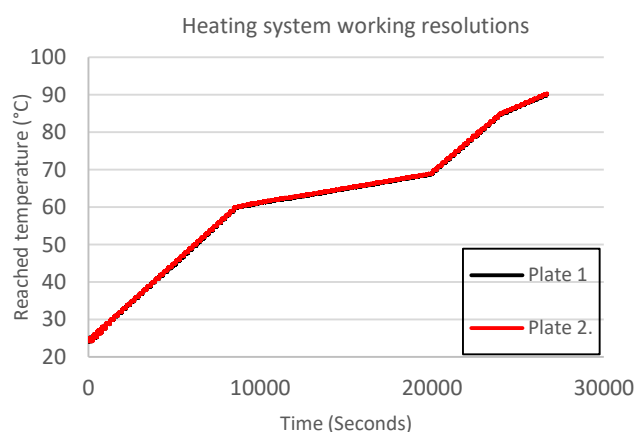
C. Heating tests

The heating system is composed of two 3.6 x 4.3 x 0.1 cm aluminum sheets that have a BI BPC 680J resistor and two type k thermocouples attached to each of them. The first thermocouple, together with the Hi 93531, works as a temporary temperature reference for the second thermocouple. It is said to be temporary because it was only used to make the correspondent temperature corrections of the second thermocouple. On the other hand, the second thermocouple is connected to an AD595 (Analog devices) that works both as a cold junction compensation system and as a thermocouple amplifier. The system output is 10mV/°C. This second subsystem is in charge of reading the heating block temperature. This signal is also used as the input for the PI controller.

Some heating tests were performed on each of the heating blocks working by separate and enclosed in a plastic case

for room temperature isolation. These tests were to observe the plates behavior and to determine if the PWM was able to produce and to read 0.2 °C temperature changes in the block temperature. After making an inspection to the obtained results, an important difference between the reference and each reading system was observed. A possible reason for this is that the Hi 93531 is a commercial precision thermometer that probably has an integrated correction circuit or makes a digital temperature correction. This suggests that some correction must be done on our system in order to increase the reading fidelity.

After analyzing the heating tests data of each block, the difference between the reference and the temperature reading system output showed a lineal behavior. There are two possible options to make the temperature correction. If it was by hardware, we would have had to implement a system capable of taking the block temperature as an input, to compare and correct point by point each reading and to give this signal as a feedback parameter to the PI controller. This would have implied to design and implement a specialized and complicated circuit, which could have had increased the production costs and the system complexity. Therefore, a digital correction was chosen as the optimal solution. By making a lineal regression of the graph, the correcting equation was obtained and the Arduino was responsible for making the point by point correction.

After the correspondent digital temperature corrections were made, the stability and functionality for each of the resolutions was tested by making a heating test on each plate working in parallel. Figure 6 shows the systems behavior for a heating test starting at 25 °C and finishing at 90°C. In this it is possible to observe that for each of the resolutions, both systems are capable of producing a stable and fine output with a 1°C/step, a 0.2°C/step and 0.5°C/step.


Figure 6. Heating test of both heating plates working in parallel and with all working resolutions. The test range was from 25°C until 90°C and the following scheme was followed: from 25 to 60 °C a 1°C/step was used, from 60 to 69 °C a 0.2°C/step, from 69 to 85°C a 1°C/step and finally from 85 to 90 °C a 5°C/step was used. The entire test took 7 hours and 30 minutes to complete.

To validate the entire system functionality, a complete heating test was performed using as template a glass slide with a microfluidic section made out of PMMA glued on top

of it. A thermocouple was attached to the glass and the complete setup was placed inside both heating plates. All data was recorded with the Arduino and the Hi 93531.

Figure 7 shows the system behavior and the glass slide temperature evolution throughout the entire test. The entire description and characterization of the system is described in Table 2. It is important to recall that there is still some small difference between the reference and the thermocouples that needs to be corrected. The heating plate 1 has a temperature error of the 3.37% while the heating plate 2 has a lower error of 1.78%. Another important thing to highlight is that the highest temperature difference between the glass slide temperature and the set point is 1.4 °C. One possible explanation for this, is that the heat transference from the plates to the glass is not completely efficient due to the big difference from the thermal conductivity coefficients of the aluminum (205W/mK) with the PMMA (0.17 W/mK) and the glass slide (1.05W/mK).
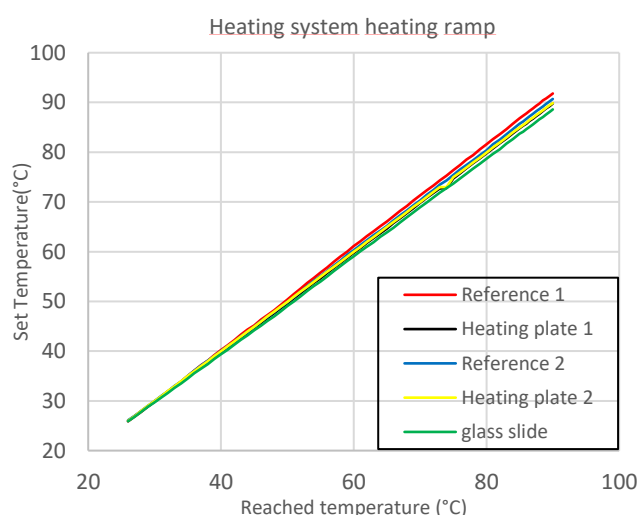
Figure 7. Heating ramp of the complete system with a glass slide – PMMA template in middle of the heating plates. The heating ramp followed the same scheme explained on **Figure 6**.

Table 2. Heating block subsystem functional parameters

Settling time (minutes)	Resolution (°C/Step)	Precision (°C)	Measurement range (°C)	Heating plate dimensions (cm)	Ramp rate (°C/min)	Cost (€)
4	0.2	0.027	25 - 96	3.6 x 4.3 x 0.1	0.05	120
4	0.5	0.027	25 - 96	3.6 x 4.3 x 0.1	0.125	120
4	1	0.027	25 - 96	3.6 x 4.3 x 0.1	0.25	120

D. Gold electrodes modification

Before making any experiments, all electrodes had to be properly cleaned following the cleaning protocol previously explained. Afterwards a cyclic voltammetry in unstirred $K_3[Fe(CN)_6]$ was performed on each electrode to determine if they were all properly cleaned. If the peak-to-peak distance was below 90 mV, the electrode was ready for modification.

In order to determine the best probe/backfiller ratio that gives the highest signal for electrochemical analysis, a polyT probe combined with DT1 was incubated on the electrode arrays. After washing the electrodes, a complimentary polyA–HRP chains are added so they can hybridize only with the polyT chains that are immobilized on the surface (because the DT1 works like a blocker on the gold surface). Finally after washing the electrodes, the system is left to react with TMB for 10 minutes and a fast chonoamperometry was performed. This experiments were done to determine the above explained, but also to define if the immobilization protocol and electrode blocking was correct.

E. Optimization of ssDNA: thiol ratio on surface for electrochemical detection.

The reason why the aforementioned model was used for the fast chronoamperometry measurements was because of the polyT complementarity with the polyA; but more importantly was because the latter is labelled with the horseradish peroxidase (HRP).

The process of detection relies on the fact that if the polyA is hybridized to the polyT on the surface. When the TMB is added in presence of the HRP, the H_2O_2 starts to oxidize the TMB, releasing two electrons for each TMB molecule and leaving the precipitate on the surface. With the fast chonoamperometry, the applied voltage pulse produces faradaic currents that are proportional to the amount of TMB that has precipitated, and hence allows to determine the optimum ssDNA: thiol ratio for the electrochemical detection.

The overall immobilization and detection process can be observed in Figure 8.
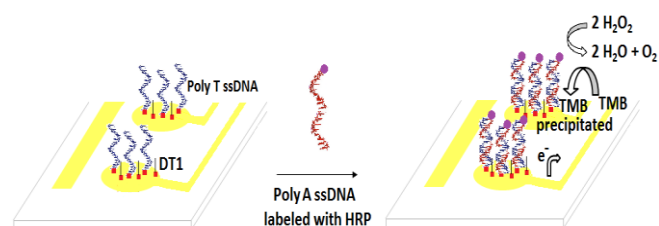
Figure 8. Schematic of electrochemical detection using a polyT, polyA-HRP, TMB/H_2O_2.

The results obtained from the fast chonoamperometric measurements show that the highest signal corresponds to the 1:1 ratio ssDNA: thiol (Figure 9). Furthermore, the signal obtained from the 1 array is one order of magnitude higher than the one obtained on the 13 array. This is due to the increased working area of this electrode, compared to the ones in the 13 array. The signal intensity dependence on the working electrodes size, is one of the mayor limiting factors for electrode miniaturization. Finally, these results demonstrate a) the good quality of manufactured electrodes and their functionality after their implementation in the fluidic system and b) and the viability of using DT1, which works well as a backfiller and blocking agent, hindering any

non-specific interaction between the surrounding medium and the gold electrodes
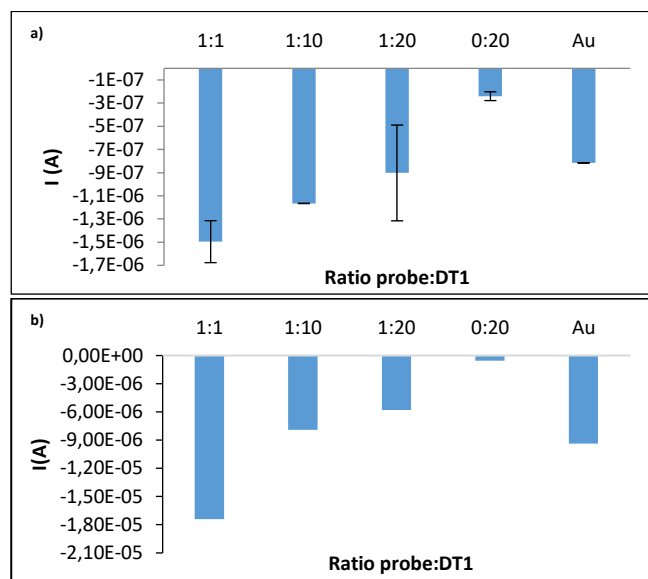
Figure 9. Fast chnoamperometric results of different ratios of probe/backfiller tested on (a) the 13 gold electrode array and on the (b) 1gold electrode array.

IV. CONCLUSIONS

When working with instrumentation systems that are intended to have a fine, appropriate and robust control of the temperature or any other variable; the controller parameters tuning is one of the most important and critical steps towards this end. After using two of the most common and recommended algebraic and practical methods: the Ziegler Nichols or the first order plus dead time (FOPDT) dynamic model, it was possible to understand and elucidate on how to properly tune each parameter depending on the desired response. However, this methods only give a rough insight of the systems response towards the tuning parameters. On the other hand, software tools like Matlab's PID tuner comes like a very handy, robust and efficient alternative for parameter tuning. This is because it not only allowed to observe in real time how the system behaved and how was the reference tracking of the controller, but it also allowed to analyze the open loop response, the controller effort, the rise time and maximum overshoot, among other parameters, in real time. This process by other means can become a time consuming and error prone endeavor due to the recalculation of each parameter by solving each equation by hand.

The development of this system shows an important technological advance since it represents one of the first examples of electronic instrumentation devices that are especially suited for electrochemically marked high-resolution melting curve analysis. Moreover, this system is capable of producing a controlled and stable output with a 1°C/step, a 0.2°C/step and 0.5°C/step resolution (parameter that can be changed whilst the process is running) with a general precision of 0.027 °C. The total production cost of this subsystem is around 120 €. Finally, this system can be furtherly improved to reduce the settling time or its resolution in order to strive for the detection of SNPs or

homozygote mutations that have neighboring complementarity. More importantly is that all the above improvements can be achieved without having the need for further image processing or bulky and complicated detection systems like the ones used for fluorescence detection.

V. FUTURE WORK

For future work the first thing that must be done is to test the system with a real and suitable biological model to perform a complete HRMCA. This will allow to further validate the systems functionality and performance and continue with the development of the other subsystems.

For the biological model the following tests are proposed: immobilize the electrodes with ssDNA probes that have different SNPs or mutations a set of electrode that contains a probe that shows no complementarity with the target and another set of blank electrodes for control testing. Next step is to produce the electrochemically marked target. One possible option is to carry on a PCR in where modified dNTPs with phenothiazine or any other electrochemically active moiety are added by the polymerase to the target DNA during the PCR. After carrying an assymetric PCR, a digestion and purification process, we should have modified a target ssDNA that will be complementary to the probes DNA carrying the different SNPs or mutations. Finally a HRMCA should be made testing all the possible resolutions and doing a first derivative method to observe and determine if there are any appreciable changes in the samples Tm or curve.

As mentioned before, the system herein explained is just one part of a complete instrumentation system. The next steps are to develop the following:

- A suitable casing to place the heating systems along with the electrodes for room temperature isolation without this hindering the connection to the reading and pumping system.
- Develop an automated pumping system that will allow to wash all the material that has not hybridized and that might contribute with background noise.
- Develop a multichannel potentiostat that could read and interface with a computer.
- This system must also be able to communicate with the processing system to ensure a proper coordination between all with the heating and pumping system.
- Develop a software that will allow to have a bidirectional communication between the user and the system as well to have a cross talking between all the subsystems.

VI. ACKNOWLEDGMENTS

VII. BIBLIOGRAPHY

[1] Z. Abdellah, A. Ahmadi y et al., "Finishing the euchromatic sequence of the human genome," Nature, vol. 431, pp. 931-945, 2004.

[2] C. F. Taylor, "mutation scanning using high resolution melting," Biochemical society transactions, vol. 37, no. 2, pp. 433-437, 2009.

[3] G. H. Fernald, E. Capriotti y et al., "Bioinformatics challenges for personalized medicine," Bioinformatics, vol. 27, nº 13, p. 1741–1748, 2011.

[4] R. M. Myers, T. Maniatis y et al., "Detection and localization of single base changes by denaturing gradient gel electrophoresis," Methods in enzymology, vol. 155, pp. 501-527, 1987.

[5] L. Zhu, H. K. Lee y et al., "Spatial temperature gradient capillary electrophoresis for DNA mutation detection," Electrophoresis, vol. 22, nº 17, p. 3683–3687, 2001.

[6] L.-S. Chou, E. Lyon and et al., "A comparison of high-resolution melting analysis with denaturing high-performance liquid chromatography for mutation scanning," American society for clinical pathology, vol. 124, pp. 330-338, 2005.

[7] G. H. Reed, J. O. Kent and et al., "High-resolution DNA melting analysis for simple and efficient molecular diagnostics," Pharmacogenomics, vol. 8, no. 6, pp. 597-608, 2007.

[8] G. H. Reed and C. T. Wittwer, "Sensitivity and specificity of single-nucleotide polymorphism scanning by high-resolution melting analysis," Clinical Chemistry, vol. 50, no. 10, pp. 1748-1754, 2004.

[9] A.-E. Surkus and G.-U. Flechsig, "Electrochemical detection of DNA Melting curves by means of heated biosensors," Electroanalysis, vol. 21, no. 10, pp. 1119-1123, 2009.

[10] K. Qamhieh, K.-Y. Wong and et al., "The melting mechanism of DNA tethered to a surface," NIH-PA, vol. 6, no. 3, pp. 474-488, 2009.

[11] X. Luo and I.-M. Hsing, "Real time Electrochemical monitoring of DNA/PNA dissociation by melting curve analysis," Electroanalysis, vol. 21, no. 14, pp. 1557-1561, 2009.

[12] S. L. Biswal, D. Raorane and et al., "Nanomechanical detection of DNA melting on microcantilever surfaces," Analytical chemistry, vol. 78, no. 20, pp. 7104-7109, 2006.

[13] R. Meunier-Prest, S. Raveau and et al., "Direct measurement of the melting temperature of supported DNA by electrochemical method," Nucleic Acids Research, vol. 31, no. 23, 2003.

[14] L. Zhou, L. Wang and et al., "High-Resolution DNA melting analysis for simultaneous mutation scanning and genotyping in solution," Clinical Chemistry, vol. 51, no. 10, pp. 1770-1777, 2005.

[15] A. V. Fotin, A. L. Drobyshev and et al., "Parallel thermodynamic analysis of duplexes on oligodeoxyribonucleotide michochips," Oxford University Press, vol. 26, no. 6, pp. 1515-1521, 1998.

[16] C. T. Wittwer, G. H. Reed and et al., "High-resolution genotyping by amplicon melting analysis using LCGreen," Clinical Chemistry, vol. 49, no. 6, pp. 853-860, 2003.

[17] D. I. Stimpson, J. V. Hoijer and et al., "Real-time detection of DNA hybridization and melting on oligonucleotide arrays by using optical wave guides," Proc. Natl. Acad. Sci., vol. 92, pp. 6379-6383, 1995.

[18] Z. Shen, H. O. Sintim and et al., "Rapid nucleic acid melting analyses using a microfabricated platform," Analytica Chimica Acta, vol. 853, pp. 265-270, 2015.

[19] N. Hany, V. Beni and et al., "Labelless electrochemical melting curve analysis for rapid mutation detection," analytical methods, vol. 2, pp. 1461-1466, 2010.

[20] H. Nasef, C. V. Ozalp and et al., "Melting temperature of surface-tethered DNA," Analytical biochemistry, vol. 406, pp. 34-40, 2010.

[21] J. B. Fiche, R. Buhot and et al., "Temperature Effects on DNA Chip Experiments from Surface Plasmon Resonance Imaging: Isotherms and Melting Curves," Biophysical journal, vol. 92, pp. 935-946, 2007.

[22] M. Liew, R. Pryor and et al., "Genotyping of Single-Nucleotide Polymorphisms by High-Resolution Melting of Small Amplicons," Clinical chemistry, vol. 50, no. 7, pp. 1156-1164, 2004.

[23] M. G. Herrmann, J. D. Durtschi and et al., "Expanded Instrument Comparison of Amplicon DNA Melting Analysis for Mutation Scanning and Genotyping," American association for clinical chemistry , vol. 53, no. 8, pp. 1544-1548, 2007.

[24] M. Li, L. Zhou and et al., "Genotyping Accuracy of High-Resolution DNA Melting Instruments," Clinical Chemistry, vol. 60, no. 6, pp. 864-872, 2014

[25] H. Cahová, L. Havran y et al., "Aminophenyl- and Nitrophenyl-Labeled Nucleoside Triphosphates:Synthesis, Enzymatic Incorporation, and Electrochemical Detection," Angewandte chemie, pp. 2089-2092, 2008.

[26] J. Balintová, L. Havran y et al., "Benzofurazane as a New Redox Label for Electrochemical Detection ofDNA: Towards Multipotential Redox Coding of DNA Bases," Chemistry European Journal, vol. 19, pp. 12720-12731, 2013.

[27] S. A. Nadeem, X. Hu y et al., "Synthesis and Characterization of pi-Stacked Phenothiazine-Labeled Oligodeoxynucleotides.," Organic letters, vol. 4, nº 26, pp. 4571-4574, 2002.

[28] S. Dulay, P. Lozano-Sanchez y et al., "Electrochemical detection of celiac disease-related anti-tissue transglutaminase antibodies using thiol based surface chemistry.,"Biosensor and Bioelectronics, vol 26, pp. 3852-3856, 2011.

[29] J. Sabaté del Rio et al. "Electrochemical detection of Francisella tularensis genomic DNA using solid-phase recombinase polymerase amplification.," Biosensors and bioelectronics, vol 54, pp. 674-678, 2014

VIII. SUPPLEMENTARY INFORMATION

Annex 1. Step response and simulated transfer function of the heating block 2 obtained with Matlab.
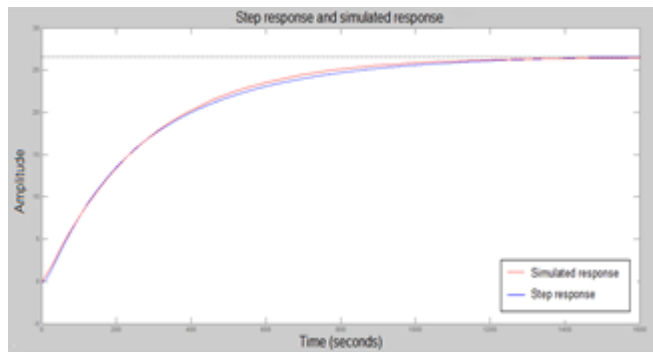
Annex 2. Modelled system of the PI controller in series with the transfer function block that simulates the behavior of the heating plate 2. Two steps where implemented as input to simulate and observe the system response to a change in the set point
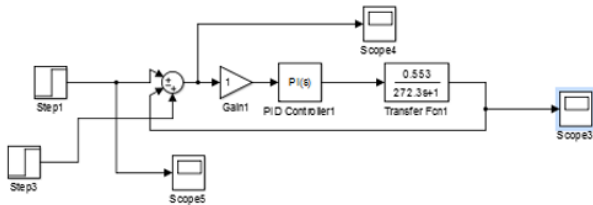
Annex 3. Modelled closed loop response of the PI controller in series with the heating block 2.